

Utilizing the Eutrophication in Bioresources Recovery and Biogas Production – A Case Study in Egypt

Mohamed M. Khalil^{1,2}, Elena Ficara², Nicola Colaninno³, Amro EL-Baz¹

¹ Environmental Engineering, Zagazig University, Zagazig 44519, Egypt

² Department of Civil and Environmental Engineering (DICA), Politecnico di Milano, Piazza Leonardo da Vinci, 32, Milan 20133, Italy

³ Department of Architecture and Urban Studies (DASTU), Politecnico di Milano, Piazza Leonardo da Vinci, 32, Milan 20133, Italy

* Corresponding author's e-mail: 10640385@polimi.it

ABSTRACT

In this work, the nutrients and eutrophication problem are integrated into a nature-based solution by incorporating microalgae-based nutrient removal from wastewater and collecting the residue in an anaerobic digestion plant to produce biogas that is directly exported to an existing gas-fired power plant and closes the bioresource loop. El Burullus lake in Egypt was selected as a case study because it is rich in nutrients and suitable for the integrated system. The theoretical results were promising as for one-hectare, nutrient pollution could be reduced with a total nitrogen removal rate of 4 kg·d⁻¹, a total phosphorus removal rate of 1.1 kg·d⁻¹, and a total COD removal rate of 9.3 kg·d⁻¹. The digester volume corresponding to the biomass produced was 120 m³ per hectare of algae pond and the methane yield (Y_{CH₄}) from anaerobic digestion was 73 m³·d⁻¹.

Keywords: eutrophication, microalgae, bioresources recovery, bioremediation.

INTRODUCTION

In the mid-20th century, eutrophication was recognized as a water pollution problem in European and North American lakes and reservoirs, resulting in three particularly disturbing ecological effects: reduced species diversity, changes in species composition and dominance, and toxic effects (Rodhe, 1969). Usually, this slow and natural eutrophication results from the discharge of N- and P-rich effluents into coastal and inland waters. Many freshwater lakes therefore suffer from algal blooms, however the same growth of microalgae can be exploited for beneficial purposes in microalgae-based wastewater treatment, as algal growth requires the addition of nutrients, mainly nitrogen, phosphorus and potassium (Slade & Bauen, 2013). This could lead to several benefits. Nutrients are recovered within the algae biomass, which is a remarkable benefit especially for phosphorus which is a finite resource that could be

depleted within 100 years, by the current usage posing a deficit starting approximately by 2070 (Demory et al., 2018). Nutrient removal costs are reduced while water is recovered for reuse and maintenance of ecological balance in aquatic and terrestrial ecosystems. To mitigate eutrophication, nutrient control is a fundamental process although there are physical and chemical methods for the removal of nutrients from wastewater, but these are costly and produce high sludge content (Boelee et al., 2011) For these reasons, the biological treatment is adapted as many species of microalgae such as *Chlorella sp.*, *Scenedesmus sp.*, and *Neochloris sp.* proven a high capacity in removing nitrogen and phosphorus from a different source of wastewater (Boelee et al., 2011). Lake Burullus in Egypt has been chosen as a case study as it is one of the vulnerable Egyptian coastal lakes that suffering from dense blue green algae, caused by discharging of eight drains into the Lake, expansion of fish farming aquaculture

(provide fish for the local market with a yield of 64,000 ton/year (Khalil, 2018) and increasing fertilizers concentration (El-Zeiny & El-Kafrawy, 2017). Lake Burullus could be classified as hypereutrophic with bad to very bad environmental conditions (Ali, 2011). Removal of nutrients from the water body is required to avoid eutrophication of this large lake. A good opportunity is offered by the cultivation of microalgae in the nutrient-rich water in high-rate algal ponds (HRAPs) where algal biomass is grown and harvested for biogas generation through anaerobic digestion process then the upgraded methane is sent to an existing gas power plant as indicated in (Figure 1).

MATERIAL AND METHODS

Lake Burullus – relevant characteristics

In this paragraph, the main characteristics of lake Burullus that are relevant to assess the feasibility of the proposed concepts are described including local climatic conditions, land availability, and the potential advantageous integrations with existing activities/infrastructures.

Climatic characteristics

Light is an important element contributing to the growth of microalgae. However, microalgae only absorb the photosynthetically active radiation (PAR), which is only 47% of the total solar spectrum. PAR varies depending on location, season and latitude. It is worth noting that solar radiation of 4 kWh/m²/d is considered sufficient for

algal production, and in areas with high solar radiation (receiving >6 kWh/m² /day), the theoretical maximum growth rate for algae is approximately 100 g/m²/day (Darzins et al., 2010), though lower experimental values are typically reported (from 2 to 25 g/m²/day for open ponds and up to 40 g/m²/day for PBR (Clippinger & Davis, 2019). Fortunately, the lake is covered by sufficient solar radiation ranging from 3.2 to 9 kWh/m²/d (Diab et al., 2015). Encouragingly, the average annual sunshine hours at our site are 3580 hours (with an average of 9 h per day) that helps providing the necessary solar coverage for algal productivity. The average annual minimum temperature is 16 °C and the average annual maximum temperature is 36 °C, which is a suitable temperature interval for most cultivated microalgal species, which ranges between 15 and 35 °C (Park et al., 2011). Moreover, as suggested by Frank Rogalla, head of R&D at Aqualia, microalgal facilities could be carried along the Mediterranean belt, including Italy, Portugal, Egypt and even South America, all of which have “favorable conditions”.

As for rainfalls, the site is characterized by moderate precipitation during the winter season with an average annual precipitation of 197.0 mm, which covers about 12.5% of the annual evaporative losses.

Land availability

One of the major limitations of microalgae cultivation in open ponds is its extensive footprint and therefore the need for large areas of land. In our case, the region has many lands unsuitable for

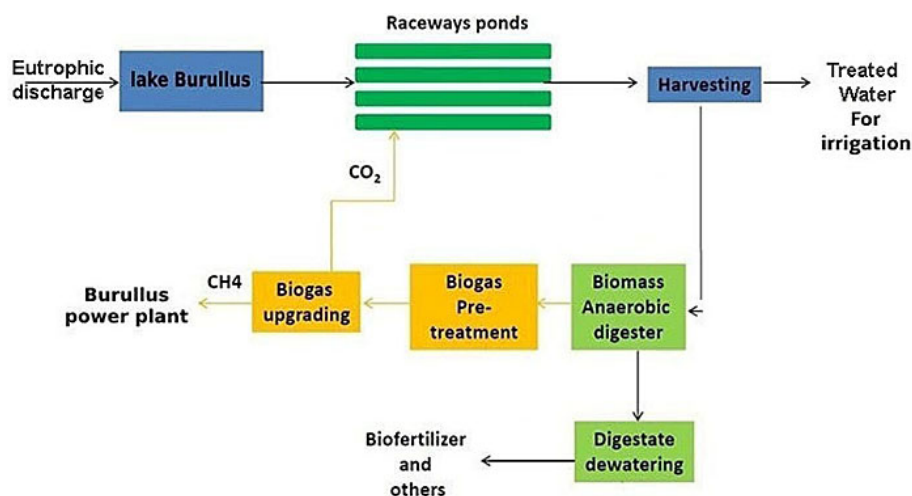


Figure 1. Simplified flow diagram for integrating HRAPs within the lake polluted water for bioresources recovering

crop production and a huge reserve of marginal and unused land. Since 1998 (Decree 1444), El Burullus Lake has been declared a protected area by the Egyptian authorities. Therefore, hundreds of kilometers are available, though it is recommended to include the ponds in the most polluted zone, which will be discussed later using remote sensing and GIS techniques.

INTEGRATIONS WITH EXISTING ACTIVITIES/INFRASTRUCTURES

Most microalgae cultivation systems attempt to maintain a moderate cultivation temperature in cool/cold weather. Therefore, the systems can adapt external heating systems, but this leads to high costs. In our case, the site is characterized by moderate temperatures throughout the year. Nevertheless, in case of need, the microalgae plant can take advantage of El Burullus power plant, which releases 5.5 m³/s of thermal water to the sea at a temperature of 35 °C. A hot water flow could be provided to the microalgae plant to regulate and control the temperature of the water and keep it within acceptable limits.

Two sources of CO₂ gas are available to supply the HRAPs with the required amount. The first source is available after the anaerobic digestion process and the upgrading of the biogas to CH₄ and CO₂. While the second source could be

applicable by connecting the HRAPs to El-Burullus power plant, which consumes 633.6 tons of gas per hour for 8 GTs (22 kg/s each) and emits up to 13 ktons of CO₂ per year, equivalent to 8.19% of Egypt's total CO₂ emissions from fuel combustion in 2000. Therefore, one or both scenarios will work together in an integrated system to mitigate the environmental impact of emission from one side and support the microalgae plant for sufficient CO₂ flow for microalgae growth and pH control from the other side.

DESIGNING OF THE EL BURULLUS MICROALGAE PLANT

Study area and strategic value

Lake El-Burullus (31° 28' 59.99" N and Longitude: 30° 51' 59.99" E) is a shallow brackish lake located between Damietta to the east and Rosetta to the west located in Kafr El-Sheikh Government and bounded on the north by Mediterranean Sea as shown in Figure 2. The lake's capacity is approximately 330 km³ and current area of 462 km² (with decreasing area and volume due to land reclamation for agriculture and aquaculture) with a length of 65 km parallel to the Mediterranean Sea shore and a width between 6 and 16 km, and a depth between 0.4 and 2 m. It is considered the second largest lake in Egypt,

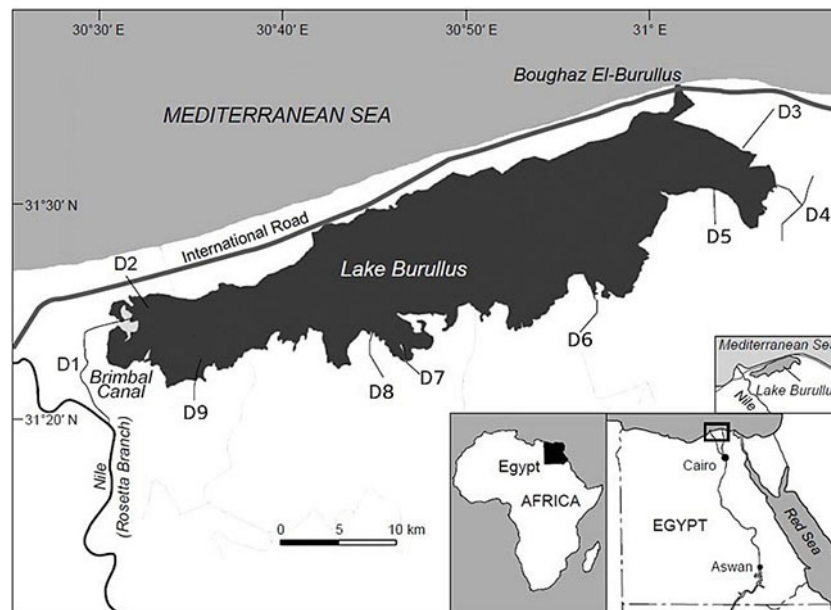


Figure 2. Map of Lake Burullus drains D1–D11. D1 – Brimbai Canal, D2 – El-Burullus West Drain, D3 – El-Burullus Drain, D4 – El-Gharbia Drain, D5 – Nasser or Tira Drain, D6 – Drain no. 6, D7 – Drain no. 7, D8 – Drain no. 8, D9 – Drain no. 9 (Ali, 2011)

connected to the Mediterranean Sea by a narrow Boughaz El-Burullus on the northeast side. As it is surrounded by farmlands, fish farms and urban areas, discharges of agricultural, domestic and industrial effluents into Lake El-Burullus have led to environmental and water system degradation. The lake receives drainage water from surrounding agricultural lands and fresh water from the Bremlal Canal. Agricultural drainage water accounts for 97% of the total inflow to the lake (4 billion m³ per year), followed by stormwater (2%) and groundwater (1%). As for the outflows, 16% of lake water evaporates and 84% flows to the sea (El-Zeiny & El-Kafrawy, 2017). In 2016, Kafr El Sheikh Wastewater Expansion Program (KESWE) was set out to reduce pollution in Mediterranean Sea by 2020 and the project is identified as a priority project under European Union's (EU) Horizon 2020 initiative. Thus, remediation is recommended by drastically reducing external nitrogen and phosphorus loads by regulating inflows from external sources (Ali, 2011). The lake is important for biodiversity conservation and a home to thousands of creatures, particularly because it provides shelter and food for migratory waterfowl, giving it the value of being defined as a Ramsar site in 1988. Ten years later, in 1998 (Decree 1444), the lake was declared a protected area by the Egyptian authorities.

Lake water characteristics

Table 1 indicates the lake water characteristics, which appear to be heavily polluted because of discharge of domestic and agricultural wastewater into the lake for decades which boosts the lake contamination.

As indicated in Figure 2, one channel (D1) and eight drains (D2-D9) discharge into the lake,

Table 1. The water characteristics of El Burullus lake (El-Zeiny & El-Kafrawy, 2017)

Parameter	Range	Average
Total nitrogen (mg/L)	12.3–26.24	18.35
Total phosphorus (mg/L)	4.4–53.7	16.55
Temperature (°C)	22–25	23.5
pH	7.5–8.8	8.2
Salinity (g/L)	0.9–13.9	4.12
DO (mg/L)	2.6–13.9	9.79
BOD (mg/L)	11.7–35.1	24.13
COD (mg/L)	62.7–423.52	151.3

therefore the mass balance describing the water and nutrient budget of the lake is as follows.

Based on these data, a mass balance describing the water trade between the lake and the surrounding area is established, according to Equation 1.

$$D + R + V_i = V_o + E \quad (1)$$

where: D – drainage water, R – rainfall, V_i – inflow water volume from the see, V_o – outflow water volume to the see, E – evaporation.

As for the meteorological data from 2019, the maximum rainfall (44.5 mm) was in December with a decreasing value until summer recorded (0 mm). Thus, the total precipitation over the lake surface during the year was 197 mm, giving a total amount of 72.5×10^6 m³. In addition, the evaporation rate was recorded as 1583 mm, corresponding to 45.7×10^6 m³ during the year. Finally, the export of water from the lake towards the Mediterranean Sea was 2.55×10^9 m³/year while the total amount of water entering the lake as a result of possible low water level was 2.03×10^9 m³/year (Ali, 2011). To calculate the concentration of nutrients in the lake water, mass balance should be carried out. As indicated in Table 2 the lake received a high amount of nutrients divided into 2150 ton/year of nitrogen and about 844 ton/year of phosphorus, which are distributed throughout the year. In addition, there is an increase of nutrients due to precipitation (33.2 tons for nitrogen and 18.3 tons for phosphorus). The exchanged water between the lake and the sea also contributes to the nutrient

Table 2. Mean monthly and total annual water (million m³) and nutrients (ton) discharged into the lake from surrounding drains in 2002–2005 (Ali, 2011)

Month	Total water budget (million m ³)	Total N budget (ton)	Total P budget (ton)
Jan	259	127.0	48.3
Feb	241	120.9	47.8
Mar	293	147.3	57.5
Apr	287	137.1	55.6
May	321	169.3	68.4
Jun	371	225.4	89.2
Jul	424	241.9	92.5
Aug	411	245.6	96.2
Sep	395	207.2	80.5
Oct	320	182.6	70.8
Nov	299	157.5	67.0
Dec	284	188.0	69.3
Total	3905	2149.8	843.1

mass balance and the annual net total of nutrients exported to the sea is 1236 tons of nitrogen and 451 tons of phosphorus as shown in Figure 3. The accumulation difference is composed of the embedded concentration in the lake water, nitrogen loss to the atmosphere, nutrient uptake by aquatic organisms and so on.

The trophic status of the lake is studied by Vollenweider chart (semi empirical statistical method, Figure 4). The following data are used:

- lake volume = 330 km³,
- lake surface $S = 410 \text{ km}^2$,

- mean depth $Z = 0.8 \text{ m}$,
- total P load $W_t = 900 \text{ tons/y}$,
- residence time $T_R = 40 \text{ days} = 0.109 \text{ y}$ (Shalby, Elshemy, Elshemy, & Zeidan, 2019).

Specific phosphorus load per unit surface of lake W_a can be calculated as follows:

$$W_a \left(\frac{g_p}{m^2 \cdot y} \right) = \frac{W_t}{S} = 2.2 \text{ g/m}^2/\text{y} \cdot \frac{Z}{T_R} = 7.34 \text{ m/y}$$

According to the Vollenweider chart the lake suffers from high eutrophic status.

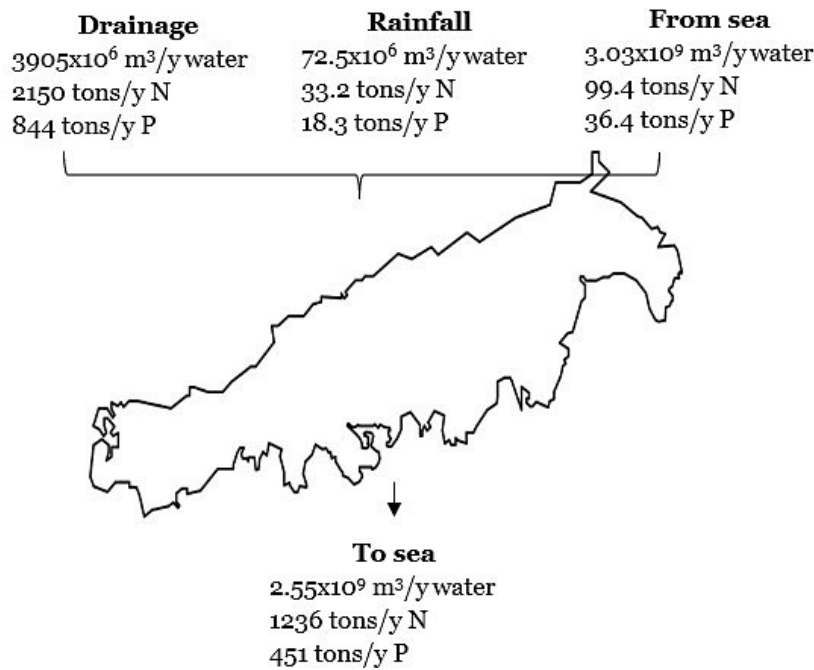


Figure 3. Mass balance for water and nutrients budget

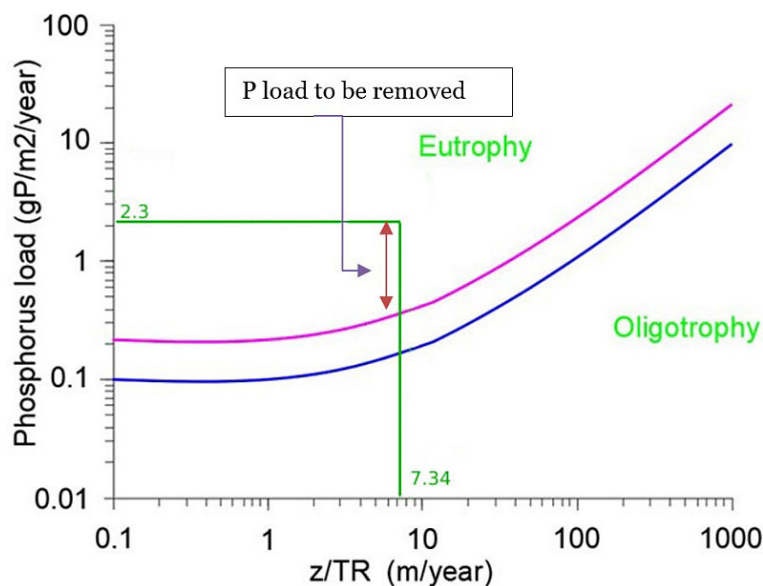


Figure 4. Vollenweider chart (semi empirical statistical method)

Assessment of water pollution in Burullus Lake using remote sensing and GIS techniques

Applications of remote sensing to eutrophication processes are adapted to describe the accumulation of nutrients that leads to excessive growth of plants and algae, causing a decrease in the penetration of sunlight into the water body. A space-based multispectral Landsat 8 OLI (Operational Land Imager) image with minimal cloud cover was freely downloaded. OLI collects data from nine spectral bands. Seven of the nine bands match Thematic Mapper (TM). Our work will mainly focus on bands 2 and 3, which are visible blue and green, respectively, as described in Table 3.

First, an August 2020 Landsat 8 image is downloaded. Then, radiometric calibration and atmospheric correction are applied to correct for atmospheric absorption and scattering. The radiometric calibration process is applied for data processing and remote sensor sensitivity, solar angle, atmospheric scattering and absorption corrections (El-Zeiny & El-Kafrawy, 2017). Then, dark object subtraction techniques (DOS) are applied to the calibrated images to remove the effect of atmospheric scattering. DOS looks for the darkest pixel value, assuming that dark objects do not reflect light; any value greater than zero must be due to atmospheric scatter. The scatter is removed by subtracting this value from each pixel in the band. This simple technique is effective for haze correction in multispectral data (Gilmore et al., 2015; El-Zeiny & El-Kafrawy, 2017).

Table 3. OLI spectral bands

Spectral Band	Wavelength	Resolution
Band 2 - Blue	0.450–0.515 μm	30 m
Band 3 - Green	0.525–0.600 μm	30 m

By using remote sensing techniques, eutrophication processes can be detected by reflectance or radiance values reflected in the signature or spectral trace. For example, clean water such as seawater tends to absorb most of the incident radiation, resulting in a black or dark blue image. In contrast, water affected by eutrophication shows high reflectivity in the green zone of the spectral signature due to the presence of chlorophyll. Water quality can be analyzed, for example, by classifying specific footprints or a spectral signature using geographic information systems such as QGIS and the semi-automatic classification plugin. As can be seen in Figure 5 for the lake El Burullus, very greenish water is observed due to the sharp increase in phytoplankton concentration in the water body.

Other ways to drill down into water quality include using regions of interest (ROIs) and spectral signatures for land cover classification to compare the spectral signature of the lake and Mediterranean Sea. From the diagram in Figure 6, it is clear that the lake is affected by the eutrophication process, which means that there is a high concentration of chlorophyll due to a higher concentration of nutrients and we can see that it has a spectral signature very similar to that of vegetation. In contrast, the Mediterranean Sea tends to absorb most of the light and the values of reflection are lower in the green range and the difference disappears significantly when it approaches the infrared range.

In addition, attempts have been made to build empirical models for detecting water quality parameters (e.g., TP, TN, and BOD) by using band combinations. Since satellite sensors are able to measure the amount of solar radiation reflected from surface water at different wavelengths,

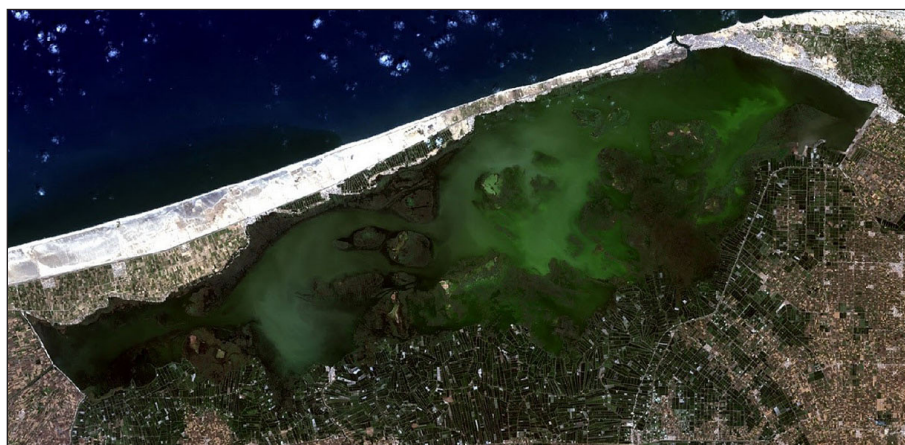


Figure 5. Greenish water due to high phytoplankton concentration, Lake El-Burullus, 2020 (Landsat 8)

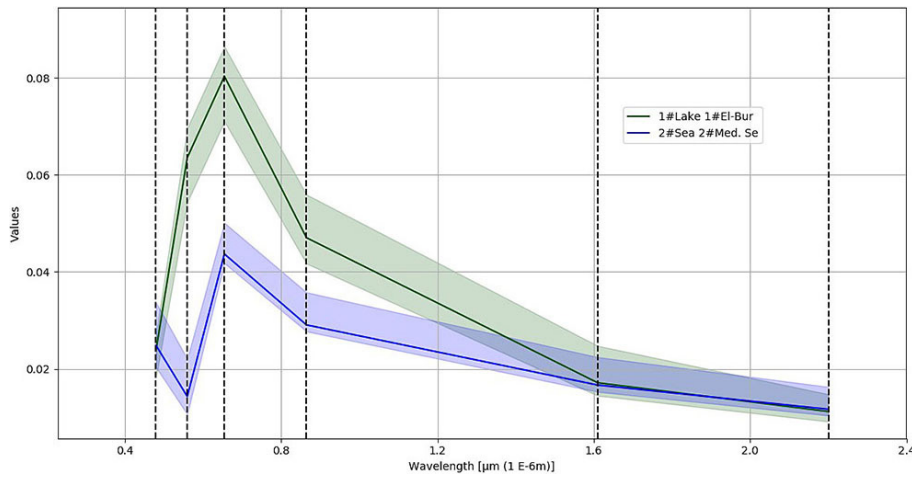


Figure 6. Spectral signature of El-Burullus lake affected by eutrophication

which can be correlated with water quality parameters, correlation matrices were created to find the statistical relationship between them. Finally, to obtain a strong model to describe the values of total nitrogen (TN), total phosphorus (TP) and biological oxygen demand (BOD), 16 band combinations were tested according to (Wang & Ma, 2001) and the following equations were developed:

$$TP (mg l^{-1}) = e^{(-0.4081-8.659*Ln(\frac{B3}{B2}))} \quad (2)$$

$$TN (mg l^{-1}) = e^{(8.228-2.713*Ln(B3+B2))} \quad (3)$$

$$BOD (mg l^{-1}) = e^{(4.2380+2.2546*Ln(\frac{(B2-B3)}{B2}))} \quad (4)$$

where: $B2$ – represent the blue band for Landsat 8 OLI, $B3$ – represent the green band for Landsat 8 OLI.

This step is fundamental to the selection of the proper area for the construction of the plant, as the lake occupies a vast area, only a few hectares are needed. These areas should be located in the most polluted zone, which are

also ideal locations for the microalgae culture plant to allow better nutrient uptake and higher and faster water reclamation. The application of remote sensing and GIS techniques help us to identify these zones as shown in Figure 7. For better description. The use of remote sensing techniques can define all indicator concentrations and the entire range of these concentrations but is only a stronger model if samples distributed along the lake are taken in the same month and year describing all indicators and calibrated with spectral data. So, in this study we will only focus qualitatively on identifying the most polluted zones. Figure 8 describes the total nitrogen where high levels of TN were detected highly in zone (3) followed by zone (2). These variations are due to the flowing drainage water, which contains high amounts of nutrients from the surrounding aquacultures (e.g., fish/shrimp ponds) in the south.

Total phosphorus, derived from Landsat OLI radiance data and plotted after processing for lower concentrations in green and higher in red, showed a large fluctuation within the lake.

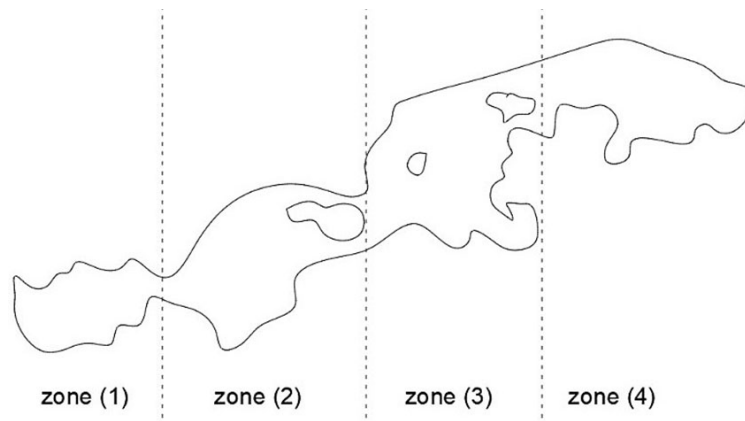


Figure 7. The lake zoning

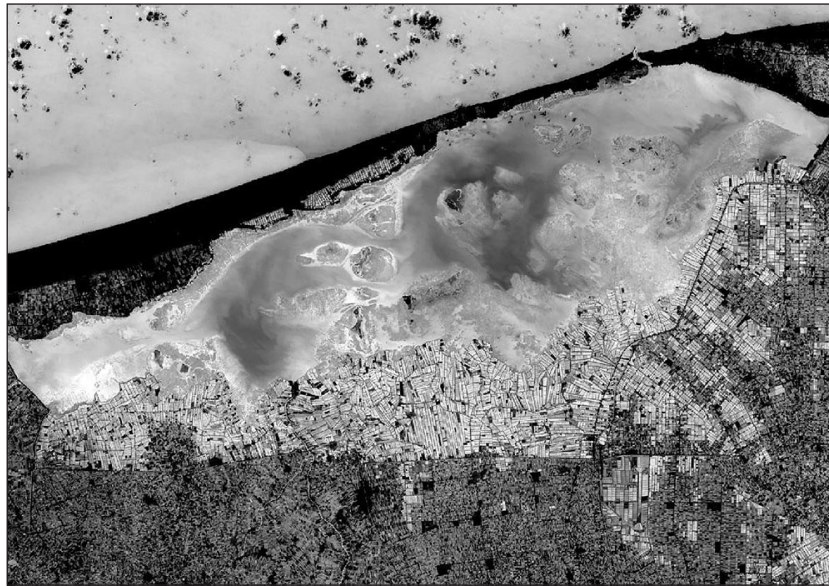


Figure 8. TN retrieved from OLI image (Aug. 2020)



Figure 9. TP retrieved from OLI image (Aug. 2020)

High values of TP were found primarily in zone (3), followed by zone (4) and then zone (2), as shown in Figure 9.

Finally, the higher BOD (Biological Oxygen Demand) indication derived from Landsat OLI radiation data is high in zone (3), followed by zone (4) and then zone (2) as shown in Figure 10.

Thus, the use of the remote sensing and GIS techniques leads to finding the suitable area for the construction of the microalgae plant for better results. By combining the three models of TP, TN and BOD, then we have the vision to decide, and this is so clear, it is zone (3) in the north next to El Burullus power plant.

PLANT DESIGN

The overall process can be divided into two modules, the first for microalgae cultivation, harvesting and dewatering, and the second for the anaerobic digester, as shown in Figure 11.

The proposed high-rate algal ponds can be located in the area between El-Burullus power station and the lake outlet on the strip between the Mediterranean Sea and the lake where the lands are available and untapped.

Furthermore, this area is next to the lake section characterized by the highest nutrients concentration ($26 \text{ mg N}\cdot\text{l}^{-1}$, $53 \text{ mg P}\cdot\text{l}^{-1}$, and $150 \text{ mg COD}\cdot\text{l}^{-1}$).

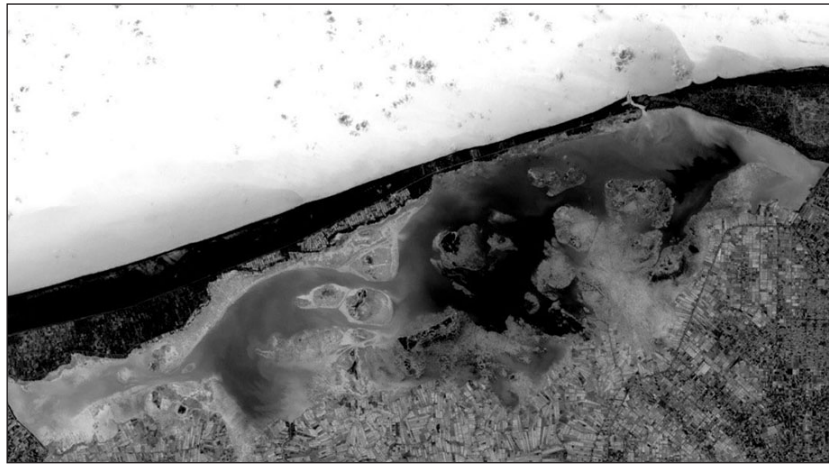


Figure 10. BOD retrieved from OLI image (Aug. 2020)

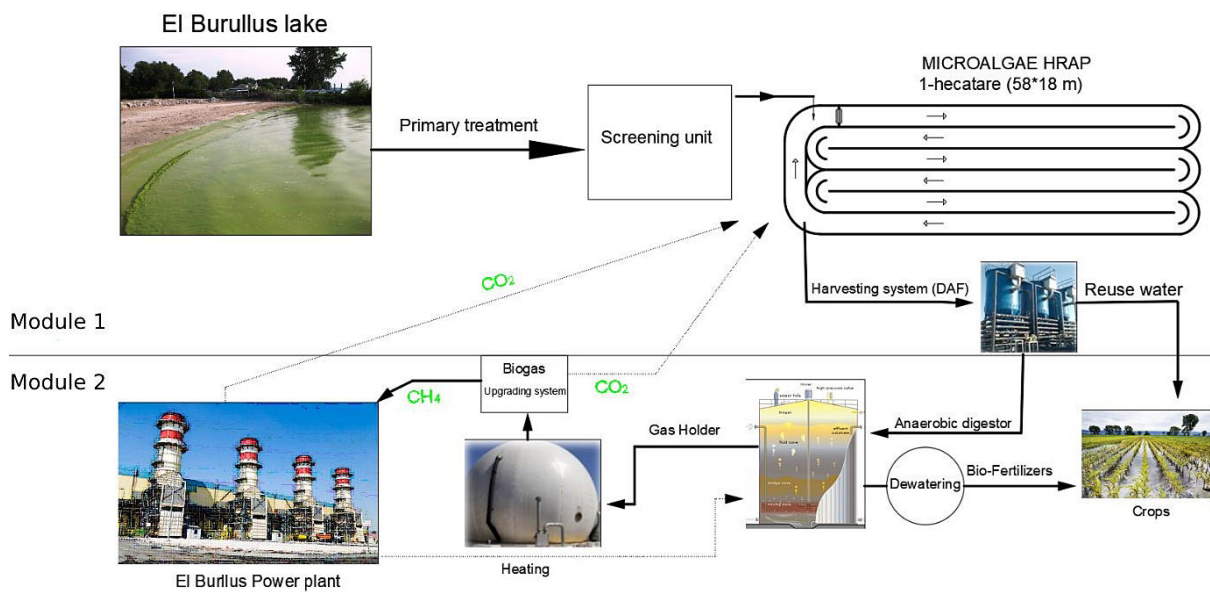


Figure 11. Layout for the entire process

Designing of the cultivation module

Based on the solar radiation, the algal productivity can be calculated as in Equation 5:

$$p_{max} = \frac{l_o * \eta_{max}}{E} \quad (5)$$

where: p_{max} – algal productivity [g/m²/d], l_o – average solar radiation [MJ/m²/d], η_{max} – maximum algal photosynthetic conversion efficiency, only (1.3–2.4%) of the total solar radiation, E – energy value of algal biomass as heat [21 kJ/g].

The average algal productivity in the lake El-Burullus is expected to be 24.2 g·m⁻²·d⁻¹. And can be computed from the solar radiation over the region and by assuming a photosynthetic efficiency of 2% and a calorific value for the algal biomass of 25.41 MJ·m⁻²·d⁻¹.

A reference 1-ha module for the HRAP is here designed, based on assumptions/guidelines taken from the literature, as summarized in Table 4.

The proposed microalgae plant in Figure 12 covers 1 hectare with a specific dimension of (58×18 m), divided by internal concrete barriers 58 m long and 3 m wide into 6 channels reaching a total length of 340 m, with the bottom lined to prevent leakage and water loss. The orientation of the HRAP should be carefully chosen to minimize wall shading. The paddle wheel maintains the velocity at 0.3 m/s. CO₂ is injected through a piping system, which comes from biogas upgrading and/or flue gas produced in the power plant El Burullus. The CO₂ is injected from the sump through fine-bubble tube aerators.

First, for a module of 1 hectare, a total wastewater volume of 500 m³/d can be treated with a

Table 4. Key assumptions used for designing the HRAP

The process	value	unit	Notes
Depth	0.25	m	From (Park et al., 2011)
Number of channels across width	6	–	–
Width of each channel	3	m	–
Average hydraulic retention time (HRT)	5	days	Varies from 3 to 6 days depending on season and weather (assumed the same as FCC Aqualia, Spain)
Linear water velocity in pond channels	0.3	m s ⁻¹	From (Park et al., 2011)
Harvesting efficiency in DAF	95	%	40 g L ⁻¹ (4%) biomass in concentrate, flocculants are used (FCC Aqualia, Spain)
Dewatering efficiency	90	%	Flocculation and centrifugation to concentrate solid biomass from 3-4% to 15-17%. Solar drier to concentrate solid biomass from 15-17% to 90% (Rogers, et al., 2014)
Nitrogen content in algae biomass	8	wt.%	Polyculture of microalgae cultivated in pre-treated wastewater (Whitton, et al., 2016)
Phosphorus content in algae biomass	2	wt.%	Ranging 0.8–2.1% by weight (Whitton, et al., 2016)

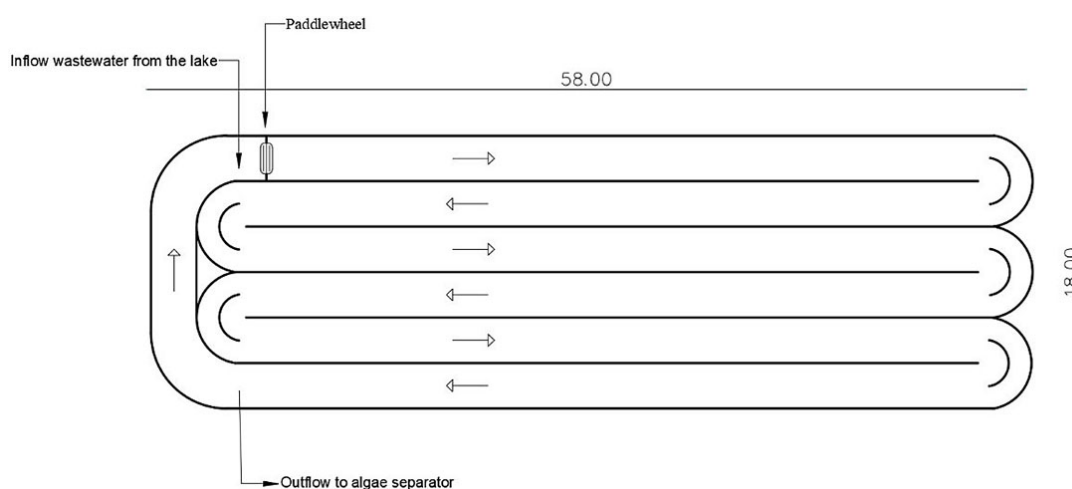


Figure 12. Schematic picture of a HRAP for 1 ha (Craggs, Sutherland, & Campbell, 2012)

volumetric loading rate (VLR) of 50 L·m⁻²·d⁻¹ calculated according to this formula:

$$VLR = \frac{Q_{in}}{A} \quad (6)$$

$$Q_{in} = \frac{A \cdot h}{HRT}$$

where: *A* – the high-rate algal pond area, 10000 m², *HRT* – hydraulic retention time, 5 days, *h* – pond height, 0.25 m, *VLR* – volumetric loading rate, 1·m⁻²·d⁻¹.

Since the evaporation value (*e*) of the lake is 3.7 (El-Geziry, 2019), the specific discharge (*Q_{out}*) is can be determined as follows:

$$Q_{out} = VLR - e \quad (7)$$

Nutrients removal rate calculations

The maximum nitrogen concentration that can be taken from the lake is 26 mg

N·l⁻¹ (El-Zeiny & El-Kafrawy, 2017) but this load alone does not support effective microalgae cultivation in HRAPs. In fact, each gram of microalgae requires 14 mg N and 6.3 mg P from new fertilizer and utilizes 42 mg N and 6.3 mg P from recovered nutrients (Frank et al., 2012). Therefore, the available N and P from the lake water would not support the expected theoretical productivity in Equation 5. Therefore, higher concentrations could be achieved by mixing the lake water with an effluent. Based on the algal productivity of 24.2 g·m⁻²·d⁻¹, the needed for sustaining microalgae growth is 45 mg/l, *C_{P,in}* is 12 mg/l are assumed as constraints to be less than 10 and 1 mg/l of total nitrogen and phosphorus respectively that fulfils the FAO for irrigation water legislation (10–15 and 2 mg/l N and P respectively). So, *C_{NH₄,out}* concentration is assumed to be 5 mg/l. As for COD, an effluent concentration of 30 mg/l is assumed, which

would depend on the stoichiometric and kinetic parameters of the heterotrophic bacteria. The design of the pond can now be done as follows.

Firstly, the N, P and COD loads are 2,2 g N·m⁻²·d⁻¹, 0.6 g P·m⁻²·d⁻¹ and 7.5 g COD·m⁻²·d⁻¹ respectively and can be calculated as follows:

$$\begin{aligned} N_{load,in} &= \frac{N_{conc} \cdot Q_{in}}{A} \\ P_{load,in} &= \frac{P_{conc} \cdot Q_{in}}{A} \\ COD_{load} &= \frac{COD_{conc} \cdot Q_{in}}{A} \end{aligned} \quad (8)$$

Hence the nitrogen removal rate NRR is 8.1 mg N·l⁻¹·d⁻¹ is and can be calculated as follows:

$$NRR = \frac{C_{NH_4,in} - C_{NH_4,out} \cdot \frac{Q_{out}}{Q_{in}}}{HRT} \quad (9)$$

Similarly, the phosphorus removal rate PRS is 2.2 mg P·l⁻¹·d⁻¹ and can be calculated as follows:

$$PRR = \frac{C_{P,in} - C_{P,out} \cdot \frac{Q_{out}}{Q_{in}}}{HRT}$$

And the same for COD removal rate is 24 mg COD·l⁻¹·d⁻¹.

$$COD_{RR} = \frac{C_{COD,in} - C_{COD,out} \cdot \frac{Q_{out}}{Q_{in}}}{HRT}$$

Kinetic models for nutrients

Currently, the most effective way to simulate wastewater treatment processes is to use the Activated Sludge Model (ASM), which has the advantage of simulating organic matter elimination along with nitrogen removal. These kinetic expressions determine the model that relates the growth rate of algae and other components to the substrate concentration in a culture medium. This is accomplished by providing equations that describe biomass production and nutrient consumption rates, which in turn can predict process performance. A steady-state calculation of the expected heterotrophic bacterial biomass is performed according to the conventional theory for biological oxidation of degradable organic matter as follows:

$$\begin{aligned} [X_B] &= \frac{STR}{HRT} \cdot \frac{Y \cdot ([S]_{IN} - [S]_{out})}{1 + b' \cdot \theta_C} \\ b' &= b_{20} \cdot \theta^{T-20} \cdot [1 - (1 - f) \cdot Y] \end{aligned} \quad (10)$$

Equation 11 describes bacteria decay (X_p), the produced inert cell debris can be quantified as follows:

$$[X_p] = f \cdot b \cdot \theta_C \cdot [X_B] \quad (11)$$

where: $[X_B]$ – concentration of heterotrophic biomass, mg TSS/l, $[X_p]$ – Inert cell debris, mg TSS/l, $[S]_{IN}$ – the soluble COD in the influent, $[S]_{out}$ – the soluble COD in the effluent, b – Decay constant at 20°C, f – fraction of inert cell debris, b' – apparent decay, K_s – half saturation constant, STR – solid's retention time, days.

Most kinetic coefficients for removal of carbonaceous material (based on bCOD) by heterotrophic bacteria and ammonia and nitrite oxidation by autotrophic bacteria are widely used in the literature (Henze, et al., 1999), as shown in Table 5.

By substituting in Equation 14, 15 and 16, and Table 6; $[S]_{IN}$ is (150 mg COD/l); $[S]_{OUT}$ is the soluble COD in the effluent from the HRAPs. For an HRT of 5 days, the expected heterotrophic biomass concentration $[X_B]$ is 43 mg VSS/l and the inert cell debris $[X_p]$ is 3.8 mg VSS/l.

For the heterotrophs, the sum of and concentrations is 58 mg VSS/l and as indicated in Table 6, the N and P content of the heterotrophs is 0.12 gN/gVS and 0.025 gP/gVS respectively, for θ_C of 5 d, they are able to assimilate 1.1 mg N·l⁻¹·d⁻¹ and 0.23 mg P·l⁻¹·d⁻¹ by substituting in Equation 12.

$$\begin{aligned} \text{Assimilated N} &= \frac{(X_B + X_p) \cdot N \text{ content}}{\theta_C} \\ \text{Assimilated P} &= \frac{(X_B + X_p) \cdot P \text{ content}}{\theta_C} \end{aligned} \quad (12)$$

According to the COD oxidation, a specific oxygen demand for heterotrophs as follows:

$$\begin{aligned} OR &= \frac{[S]_{IN} - [S]_{out}}{\theta_H} (1 - Y) + \\ &+ (1 - Y) \cdot b_{20} \cdot \theta^{T-20} \cdot [X_B] \cdot (1 - f) \end{aligned} \quad (13)$$

By substitution, the oxygen demand OR is 9.5 mg O₂·l⁻¹·d⁻¹. In terms of algal biomass, it can be calculated as follows:

$$X_A = \frac{p_{max} (gVSS/m^2/d)}{h_{pond}} * \theta_C \quad (14)$$

Assuming that the limiting factor for algal growth is light availability, the algal biomass X_A is 486 mg VSS·l⁻¹. Oxygen production by microalgae can be estimated as follows:

$$OP = X_A \cdot \alpha O_2 / \theta_C \quad (15)$$

where: αO_2 – is the specific oxygen production per unit of algal biomass produced (1.57 g O₂·g⁻¹ VSS) (Ji, et al., 2015); this gives of 146 mg O₂·l⁻¹·d⁻¹.

Table 5. Kinetic coefficients for BOD removal and nitrification at 20°C

Coefficient	Unit	COD oxidation	NH ₄ oxidation	NO ₂ oxidation
μ_{max}	1/d	6	0.9	1
K_S, K_{NH_4}, K_{NO_2}	mg/L	8	0.5	0.2
b	g VSS/g VSS-d	0.12	0.17	0.17
f	Unitless	0.15	0.15	0.15
K_{O_2}	mg/L	0.2	0.5	0.9
Temperature correction factors				
μ_{max}	Unitless	1.07	1.072	1.063
b	Unitless	1.04	1.029	1.029

Table 6. Stoichiometry composition of biomasses

Specification	Algae	Nitrifiers	Heterotrophs
N content gN/gVS	0.08	0.12	0.12
P content gP/gVS	0.02	0.02	0.025
O ₂ request	–	4.33 gO ₂ /gNrem 4.57 gO ₂ /gNox	1.13 gO ₂ /gVS 0.53 gO ₂ /gCOD
O ₂ production	1.5 gO ₂ /gVS	–	–
Growth yield	–	0.16 gVS/gNox	0.45 gTS/gCOD

The N and P content of the algae is 0.07 gN/gVS and 0.02 gP/gVS respectively, for θ_c of 5 d, they are able to assimilate 6.8 mg N·l⁻¹·d⁻¹ and 1.9 mg P·l⁻¹·d⁻¹.

$$Assimilated\ N = \frac{X_A \cdot N\ content}{\theta_c}$$

$$Assimilated\ P = \frac{X_A \cdot P\ content}{\theta_c}$$

Finally, the total suspended solids production TSS which includes all heterotrophs, nitrifiers, and algal biomasses is 575 mg·l⁻¹ and can be calculated as follows:

$$TSS = (X_B + X_P + X_A) \cdot \frac{Q_{in}}{Q_{out}} \quad (16)$$

The TSS production rate for 1 hectare HRAP is 287 kg·d⁻¹ as follows:

$$TSS_{out} = \frac{TSS \cdot Q}{\theta_c} \quad (17)$$

One hectare of microalgae pond can treat 500 m³·d⁻¹ and produces about 287 kg TSS·d⁻¹, which is about 105 tons of dry biomass per year, assuming that 50% is anaerobically digested, as in Aqualia, Spain. The remaining biosolid as fertilizer is more than 50 t TS /ha/year.

The net oxygen production rate OP_{net} is 136 O₂ l⁻¹·d⁻¹ and represent the difference between the microalgae production rate OP and the consumption of heterotrophs OR_H

$$OP_{net} = OP - OR_H \quad (18)$$

It is also possible to perform a CO₂ mass balance. First the CO₂ production rate by heterotrophs (CP) is compute as follows:

$$CP = OP \cdot \alpha CO_{2_O_2} \quad (19)$$

where: $\alpha CO_{2_O_2}$ – the average ratio between O₂ consumption and CO₂ production (taken as 1.375 g CO₂/gO₂ equal to the molar oxygen demand for carbohydrate oxidation (Marazzi et al., 2020). This results in a CO₂ production rate (CP) of 13.7 mg CO₂·l⁻¹·d⁻¹.

In contrast, microalgae consume CO₂ according to a stoichiometric need of 1.88 g CO₂/g TSS. Then, the CO₂ consumption rate of microalgae is:

$$CR = \frac{X_A}{HRT} \cdot \alpha CO_2 \quad (20)$$

Net CO₂ consumption is the difference between the consumption of microalgae and the production of heterotrophs, which is equal to 183 mg CO₂·l⁻¹·d⁻¹. This result suggests that CO₂ supply is required to support microalgal growth.

The performance of the system in terms of nutrients removal rate N_{uptake} and P_{uptake} are 8 mg N·l⁻¹·d⁻¹ and 2.2 mg P·l⁻¹·d⁻¹ respectively, and can be calculated as follows:

$$N_{uptake} = \sum Assimilated\ N_H + Assimilated\ N_A$$

$$P_{uptake} = \sum Assimilated\ P_H + Assimilated\ P_A \quad (21)$$

Finally, the effluent characteristics for both nitrogen concentration ($C_{NO_3,out}$) and phosphorus

concentration are $1 \text{ mg NO}_3 \cdot \text{l}^{-1}$ and $(C_{P,out})$ respectively, and can be calculated as follows:

$$C_{NO3,out} = (NRR \cdot \theta_C - N_{\text{uptake}} \cdot \theta_C) \cdot \frac{Q_{in}}{Q_{out}}$$

$$C_{P,out} = (C_{P,in} - P_{\text{uptake}} \cdot \theta_C) \cdot \frac{Q_{in}}{Q_{out}} \quad (22)$$

The overall HRAP contribution to the lake nutrient removal would eventually depend on the available land. The project area can be scaled to 1000 ha according to available water and nutrient budget.

Designing on the anaerobic digestion plant

Main assumptions in the design of the AD section are reported in Table 7. A digester with volume of is determined based on the organic loading rate (OLR) and the harvested algae concentration X_A of $100 \text{ kg} \cdot \text{m}^{-3}$ as follows:

$$V_d = \frac{TSS_{out} \cdot \left(\frac{\text{COD}}{\text{TS}}\right)}{OLR} \quad (23)$$

The hydraulic retention time is 42 d and it is computed according to this formula:

$$Q_{in} = \frac{TSS}{x_A}$$

$$HRT = \frac{V_d}{Q_{in}} \quad (24)$$

Finally, the 120 m^3 thermophilic anaerobic sludge digester is cylindrically shaped and well mixed with a mechanical mixer, with a gas and sludge outlet as shown in Figure 13.

The design of the digester volume should consider the total suspended solids content of the lake, which according to Environmental Monitoring Program for Egyptian Lakes, 2017, ranges from 37 mg/l to 148 mg/l . So, the volume of the biogas plant can be increased. But it is not possible to be handled in this study because we miss its anaerobic degradability.

Expected energy recovery

The methane yield (Y) from anaerobic digestion of microalgae was taken as $0.256 \text{ l CH}_4/\text{g VSS}$ as the minimum value obtained in the thermophilic process and after thermal pretreatment (Uggetti et

Table 7. Key assumptions and model details of the AD

The process	Value	Unit	Notes
Digester working temperature	55	°C	Thermophilic approach (heat available from El-Burullus power plant)
Algae slurry temperature	18	°C	The average annual temperature in the area varies between 16°C and 36 °C
Organic loading rate (OLR)	3.5	kg COD m ⁻³ d ⁻¹	The optimal anaerobic digestion is 1.6-4.8 kg TS m ⁻³ ·d ⁻¹ (Rittmann 1, 2001).
COD/TS ratio for algal biomass	1.5	g/g	–
Pre-treatment (thermal pre-treatment)	120	°C	The methane yield is increased by 93% (Uggetti, et al., 2017)
Methane yield from anaerobic digestion	0.256	L CH ₄ /g VS ⁻¹	Assumed to be the minimum value obtained in the thermophilic process and after thermal pre-treatment (Uggetti, et al., 2017)

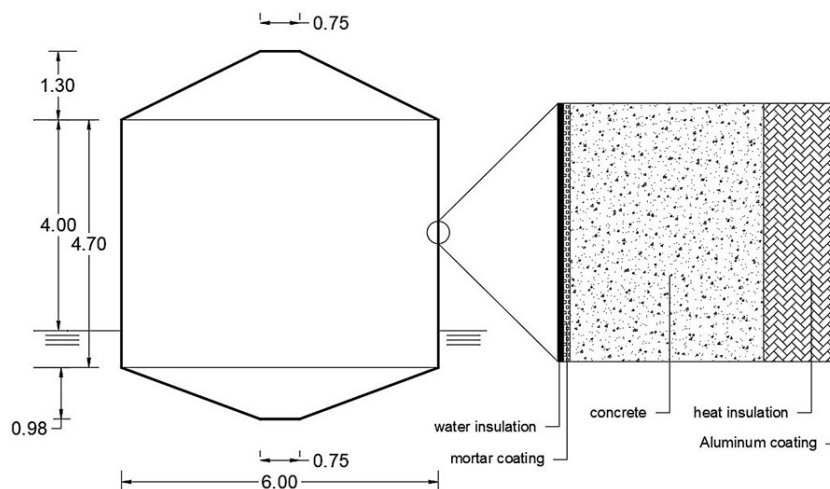


Figure 13. The anaerobic digester geometric shape and insulation details

al., 2017). It is worth noting that (Ward et al., 2014) in their study found that the biomass of most algal species is almost more than 90% volatile solids (VS), which allows the assumption that TSS is almost equal to VSS. Then the overall potential methane yield is $73 \text{ m}^3 \cdot \text{d}^{-1}$ according to this formula:

$$Q_{CH_4, produced} \left(\frac{\text{m}^3 \cdot \text{atm}}{\text{d}} \right) = F_{VS} \cdot Y \quad (25)$$

CONCLUSIONS

In this study, the integration of pollution into bioresource utilization was carried out, microalgae-based nutrient removal from wastewater serves the dual purpose of bioremediation of eutrophication phenomena in the lake El-Burullus plus beneficial algal biomass production in a closed loop. The mass and energy flux for the 1-ha installation are evidence of the ability of microalgae to remove nutrients and the feasibility of scaling the project to hundreds of high-rate algal ponds (HARPs) based on nutrient and water budgets and available area. The study area meets the requirements for microalgae cultivation due to sunny weather, availability of land and wastewater, and the possibility of taking advantage of the existing power plant. Assessment of phosphorus concentration P in EL-Burullus Lake, Egypt using Landsat 8 operational land imager and GIS techniques can detect the most polluted zones based on an empirical model of band combinations. Accordingly, the location of HRAPs is chosen. For one-hectare, nutrient pollution could be reduced with a total nitrogen removal rate of $4 \text{ kg} \cdot \text{d}^{-1}$, a total phosphorus removal rate of $1.1 \text{ kg} \cdot \text{d}^{-1}$, and a total COD removal rate of $9.3 \text{ kg} \cdot \text{d}^{-1}$. Microalgae cultivation contributes to carbon dioxide reduction as each cultivated hectare can absorb carbon dioxide up to $183 \text{ mg mg CO}_2 \cdot \text{l}^{-1} \cdot \text{d}^{-1}$ and emits oxygen of about $136 \text{ mg mg O}_2 \cdot \text{l}^{-1} \cdot \text{d}^{-1}$. One hectare of microalgae pond can process $500 \text{ m}^3 \cdot \text{d}^{-1}$ producing more than 50 t TS /year of biosolids residues as fertilizer. The digester volume corresponding to the biomass produced is 120 m^3 per hectare of algae pond and the methane yield from anaerobic digestion is $73 \text{ m}^3 \cdot \text{d}^{-1}$.

REFERENCES

1. Ali, E.M. 2011. Impact of drain water on water quality and eutrophication status of Lake Burullus, Egypt, a southern Mediterranean lagoon. *African Journal of Aquatic Science*, 36(3), 267–277. Retrieved from <https://tandfonline.com/doi/abs/10.2989/16085914.2011.636897>
2. Boelee, N.C., Temmink, H., Janssen, M., Buisman, C.J., Wijffels, R.H., & Boelee et al., 2011. Nitrogen and phosphorus removal from municipal wastewater effluent using microalgal biofilms. *Water Research*, 45(18), 5925–5933.
3. Clippinger, J.N., & Davis, R.E. 2019. Techno-economic analysis for the production of algal biomass via closed photobioreactors: future cost potential evaluated across a range of cultivation system designs. *National Renewable Energy*.
4. Craggs, R.J., Sutherland, D.L., Campbell, H. 2012. Hectare-scale demonstration of high rate algal ponds for enhanced wastewater treatment and biofuel production. *Journal of Applied Phycology*, 24(3), 329–337. Retrieved from <https://link.springer.com/article/10.1007/s10811-012-9810-8>
5. Darzins, A., Pienkos, P., Edye, L. 2020. Current status and potential for algal biofuels production. *IEA Bioenergy Task 39*. Retrieved from <http://task39.org/files/2013/05/IEA-Task-39-Current-Status-and-Potential-of-Algal-biofuels0.pdf>
6. Demory, Combe, C., Hartmann, P., Talec, A., Pruvost, E., Hamouda, R. Demory et al., 2018. Supplementary material from “How do microalgae perceive light in a high-rate pond? Towards more realistic Lagrangian experiments”. Retrieved from https://rs.figshare.com/collections/supplementary_material_from_how_do_microalgae_perceive_light_in_a_high-rate_pond_towards_more_realistic_lagrangian_experiments_/4100834
7. Diab, F., Lan, H., Zhang, L., Ali, S. 2015. An Environmentally-Friendly Tourist Village in Egypt Based on a Hybrid Renewable Energy System—Part One: What Is the Optimum City? *Energies*, 8(7), 1-19. Retrieved from <https://mdpi.com/1996-1073/8/7/6926/pdf>
8. El-Geziry, E.A. 2019. water and nutrients budget of lake Burullus, Egypt. *Blue Biotechnology Journal*.
9. El-Zeiny, A.M., & El-Kafrawy, S. B. 2017. Assessment of water pollution induced by human activities in Burullus Lake using Landsat 8 operational land imager and GIS. *The Egyptian Journal of Remote Sensing and Space Science*, 20. Retrieved from <https://sciencedirect.com/science/article/pii/S1110982316300680>
10. Frank, E.D., Han, J., Palou-Rivera, I., Elgowainy, A., Wang, M. 2012. Methane and nitrous oxide emissions affect the life-cycle analysis of algal biofuels. *Environmental Research Letters*, 7(1), 014030. Retrieved from <https://greet.es.anl.gov/files/ch4-nox-algal-biofuels>
11. Gilmore, S., Saleem, A., Dewan, A. 2015. Effectiveness of DOS (Dark-Object Subtraction) method and

- water index techniques to map wetlands in a rapidly urbanising megacity with Landsat 8 data. Retrieved from <http://ceur-ws.org/vol-1323/paper41.pdf>
12. Henze, M., Gujer, W., Mino, T., Matsuo, T., Wentzel, M.C., Marais, G., Loosdrecht, M.C. 1999. Activated Sludge Model No.2d, ASM2D. *Water Science and Technology*, 39(1), 165-182. Retrieved from <https://sciencedirect.com/science/article/abs/pii/S0273122398008294>
 13. Ji, M.K., Yun, H.S., Park, S., Lee, H., Park, Y.T., Bae, S., Choi, J. 2015. Effect of food wastewater on biomass production by a green microalga *Scenedesmus obliquus* for bioenergy generation. *Bioresource Technology*, 179, 624-628. Retrieved from <https://sciencedirect.com/science/article/pii/S0960852414017994>
 14. Khalil, M.T. 2018. Fisheries of Egyptian Delta Coastal Wetlands; Burullus Wetland Case Study. Retrieved from https://link.springer.com/chapter/10.1007/698_2017_204
 15. Marazzi, F., Bellucci, M., Ficara, E., Mezzanotte, V. 2020. Interactions between Microalgae and Bacteria in the Treatment of Wastewater from Milk Whey Processing. *Water*.
 16. Park et al. 2011. Wastewater treatment high rate algal ponds for biofuel production. *Bioresource Technology*, 102(1), 35–42. Retrieved from <https://sciencedirect.com/science/article/pii/S0960852410011636>
 17. Rittmann, M.Z. 2001. *Environmental Biotechnology*. McGraw Hill. Retrieved 9 30, 2020
 18. Rodhe, W. 1969. Crystallization of eutrophication concepts in northern Europe. Retrieved from <https://eurekamag.com/research/026/348/026348261.php>
 19. Rogers, J.N., Rosenberg, J.N., Guzman, B.J., Oh, V.H., Mimbela, L.E., Ghassemi, A., Donohue, M.D. 2014. A critical analysis of paddlewheel-driven raceway ponds for algal biofuel production at commercial scales. *Algal Research-Biomass Biofuels and Bioproducts*, 4, 76-88. Retrieved from <https://sciencedirect.com/science/article/pii/S2211926413001008>
 20. Shalby, A., Elshemy, M., Elshemy, M., Zeidan, B.A. 2019. Assessment of climate change impacts on water quality parameters of Lake Burullus, Egypt. *Environmental Science and Pollution Research*, 1-22. Retrieved from <https://link.springer.com/article/10.1007/s11356-019-06105-x>
 21. Slade, R., Bauen, A. 2013. Micro-algae cultivation for biofuels: Cost, energy balance, environmental impacts and future prospects. *Biomass & Bioenergy*, 53, 29–38. Retrieved from <https://sciencedirect.com/science/article/pii/S096195341200517x>
 22. Uggetti, E., Passos, F., Passos, F., Solé, M., Garfi, M., Ferrer, I. 2017. Recent Achievements in the Production of Biogas from Microalgae. *Waste and Biomass Valorization*, 8(1), 129–139. Retrieved from <https://link.springer.com/article/10.1007/s12649-016-9604-3>
 23. Wang, Ma, A. 2001. Application of Remote Sensing Techniques in Monitoring and Assessing the Water Quality of Taihu Lake. *Bulletin of Environmental Contamination and Toxicology*.
 24. Ward, A.J., Lewis, D., Green, F. 2014. Anaerobic digestion of algae biomass: A review. *Algal Research-Biomass Biofuels and Bioproducts*, 5(1), 204–214. Retrieved from <https://sciencedirect.com/science/article/pii/S2211926414000216>
 25. Whitton, R., Mével, A. L., Pidou, M., Ometto, F., Villa, R., Jefferson, B. 2016. Influence of microalgal N and P composition on wastewater nutrient remediation. *Water Research*, 91, 371–378. Retrieved from <https://sciencedirect.com/science/article/pii/S0043135415304528>